

# Revising a process-based biogeochemistry model (DNDC) to simulate methane emission from rice paddy fields under various residue management and fertilizer regimes

TAMON FUMOTO\*, KAZUHIKO KOBAYASHI†, CHANGSHENG LI‡, KAZUYUKI YAGI\* and TOSHIHIRO HASEGAWA\*

\*National Institute for Agro-Environmental Sciences, Kannondai 3-1-3, Tsukuba 305-8604, Japan, †University of Tokyo, Yayoi 1-1-1, Bunkyo-ku, Tokyo 113-8657, Japan, ‡Institute for the Study of Earth, Oceans and Space, University of New Hampshire, Durham, NH 03824, USA

## Abstract

A comprehensive biogeochemistry model, DNDC, was revised to simulate crop growth and soil processes more explicitly and improve its ability to estimate methane (CH<sub>4</sub>) emission from rice paddy fields under a wide range of climatic and agronomic conditions. The revised model simulates rice growth by tracking photosynthesis, respiration, C allocation, tillering, and release of organic C and O<sub>2</sub> from roots. For anaerobic soil processes, it quantifies the production of electron donors [H<sub>2</sub> and dissolved organic carbon (DOC)] by decomposition and rice root exudation, and simulates CH<sub>4</sub> production and other reductive reactions based on the availability of electron donors and acceptors (NO<sub>3</sub><sup>-</sup>, Mn<sup>4+</sup>, Fe<sup>3+</sup>, and SO<sub>4</sub><sup>2-</sup>). Methane emission through rice is simulated by a diffusion routine based on the conductance of tillers and the CH<sub>4</sub> concentration in soil water. The revised DNDC was tested against observations at three rice paddy sites in Japan and China with varying rice residue management and fertilization, and produced estimates consistent with observations for the variation in CH<sub>4</sub> emission as a function of residue management. It also successfully predicted the negative effect of (NH<sub>4</sub>)<sub>2</sub>SO<sub>4</sub> on CH<sub>4</sub> emission, which the current model missed. Predicted CH<sub>4</sub> emission was highly sensitive to the content of reducible soil Fe<sup>3+</sup>, which is the dominant electron acceptor in anaerobic soils. The revised DNDC generally gave acceptable predictions of seasonal CH<sub>4</sub> emission, but not of daily CH<sub>4</sub> fluxes, suggesting the model's immaturity in describing soil heterogeneity or rice cultivar-specific characteristics of CH<sub>4</sub> transport. It also overestimated CH<sub>4</sub> emission at one site in a year with low temperatures, suggesting uncertainty in root biomass estimates due to the model's failure to consider the temperature dependence of leaf area development. Nevertheless, the revised DNDC explicitly reflects the effects of soil electron donors and acceptors, and can be used to quantitatively estimate CH<sub>4</sub> emissions from rice fields under a range of conditions.

*Keywords:* biogeochemical modeling, decomposition, electron donors, global warming, greenhouse gases, methane emission, *Oryza sativa*, paddy fields, rice, soil redox status

*Received 5 January 2006; revised version received 8 May 2007 and accepted 23 July 2007*

## Introduction

The atmospheric concentration of methane (CH<sub>4</sub>), a potent greenhouse gas, has increased from 0.75 ppmv during the preindustrial period to a current value of

1.73 ppmv (Lelieveld *et al.*, 1998). As radiative forcing by CH<sub>4</sub> is 21 times that of CO<sub>2</sub> over a 100-year time horizon (Lashof & Ahuja, 1990), the contribution of CH<sub>4</sub> to global warming is estimated to be about 10% of that produced by CO<sub>2</sub>. Rice paddy fields are a major source of global CH<sub>4</sub> emission: according to an estimate by IPCC (1995), these fields contribute 11% (60 Tg yr<sup>-1</sup>) of global CH<sub>4</sub> emissions. However, the range in this

Correspondence: Tamon Fumoto, tel./fax: +81 29 838 8330, e-mail: tamon@niaes.affrc.go.jp

estimate is wide (20–100 Tg yr<sup>-1</sup>), largely due to uncertainties in estimates of CH<sub>4</sub> emission under a variety of environmental and agronomic conditions (e.g. climate, soil types, rice cultivars, farming practices). As it is impossible to measure CH<sub>4</sub> emissions from paddy fields under all possible conditions, global estimates of CH<sub>4</sub> emission must rely on modeling to scale up emission estimates from local samples and to evaluate potential mitigative measures.

In paddy soils, CH<sub>4</sub> is produced by methanogens through anaerobic decomposition of organic matter, and part of the CH<sub>4</sub> is oxidized by methanotrophic bacteria in aerobic regions of the soil (i.e. the surface soil layer and the rice rhizosphere). Methane stored in soil can be emitted to the atmosphere via three pathways: diffusion through flood water, ebullition, and transport through rice plants. Of these pathways, transport through rice plants is the most important: several studies have estimated that about 90% of CH<sub>4</sub> emission during the rice growing season occurred through rice plants (Schütz *et al.*, 1991; Butterbach-Bahl *et al.*, 1997). Therefore, models capable of predicting CH<sub>4</sub> emissions must properly simulate the processes of CH<sub>4</sub> production, oxidation, and transport through rice plants.

DNDC is a comprehensive biogeochemistry model that simulates crop growth and soil C and N dynamics based on input data on soil properties, climate, and farming practices (e.g. Li *et al.*, 1992, 1994). Following its early development, the model was expanded to simulate the emission of trace gases such as NO, N<sub>2</sub>O, NH<sub>4</sub>, and CH<sub>4</sub> from agricultural ecosystems and natural wetlands (Zhang *et al.*, 2002; Li *et al.*, 2004). To test its ability to predict CH<sub>4</sub> emission from rice fields, DNDC was supplied with site-scale observations from the United States, China, Thailand, and India (Li, 2000; Li *et al.*, 2002; Cai *et al.*, 2003; Babu *et al.*, 2006). In these studies, predicted seasonal CH<sub>4</sub> emission generally agreed well with observations. However, the model's ability to predict shorter-term temporal emission patterns was less successful, irrespective of whether or not the total emission was predicted well. In the Indian examples (Babu *et al.*, 2006), calibration of a model parameter (the microbial activity index) was necessary to reduce the simulated emissions to a level comparable to observed values. These results suggested that DNDC required further revision to improve its ability to predict CH<sub>4</sub> emissions in a range of environments.

One of the limitations of the current DNDC model, with respect to the wet and dry cycle experienced by paddy fields is the model's dependence on empirical simulation of changes in a soil's redox potential (*Eh*), which acts as a major driver for CH<sub>4</sub> production but does not account for changes in the availabilities of electron donors [e.g. dissolved organic carbon (DOC)

and H<sub>2</sub>] and acceptors (e.g. Fe<sup>3+</sup>). Consequently, the model's simulation of soil *Eh* is insensitive to the amounts of various oxidants, which should have a significant influence on changes in soil *Eh*. In addition, the current version of DNDC lacks a proper method for estimating soil thermal environments: it assumes that the soil surface temperature equals the air temperature, but in reality, the temperatures of air and water or soil can differ greatly, introducing another source of error in the rates of temperature-dependent soil processes. Third, the current version of DNDC does not include aspects of plant C metabolism, such as photosynthesis, respiration, and C allocation among organs, which have large impacts on CH<sub>4</sub> production and emission. In this study, we attempted to make substantial modifications to DNDC's submodels of soil climate, crop growth, and soil biogeochemistry to improve its performance across a range of climatic, soil, and management conditions. The revised model was then tested against observations at several rice fields in Japan and China.

### Outline of the model revision

As described in previous publications (e.g. Li *et al.*, 1992; Li, 2000), DNDC consists of three major submodels: soil climate, crop growth, and soil biogeochemistry. The soil climate submodel calculates moisture, temperature, and O<sub>2</sub> concentration in the soil based on inputs of soil properties and weather conditions. The crop growth submodel simulates crop physiology and phenology based on the environment above and below the ground and on N availability. Crop growth is fed back into the soil climate submodel through water uptake, and is linked to the soil biogeochemistry submodel through N uptake and the supply of organic C by plants. The soil biogeochemistry submodel simulates various biogeochemical processes in soil as a function of soil properties and climate. Soil biogeochemistry is fed back into crop growth through its effects on N availability. In this study, we developed major revisions to the crop growth and soil biogeochemistry submodels. We also moderately revised the soil climate submodel to simulate water and soil temperatures in flooded fields. Specific descriptions of the revised DNDC are provided in the Appendix A.

### Crop growth

In our revision of the crop growth submodel, we incorporated MACROS (Penning de Vries *et al.*, 1989), an established model of crop carbon metabolism, to explicitly describe photosynthesis subject to N availability and atmospheric CO<sub>2</sub> concentration, respiration, and C allocation. Carbon flux from plant roots to soil in

the form of respiration, turnover of organic matter, and exudation are all parts of a crop's carbon balance; hence, the revised model now directly links CH<sub>4</sub> production with plant C metabolism. In addition, CH<sub>4</sub> oxidation and transport are explicitly described by accounting for O<sub>2</sub> release from the roots and CH<sub>4</sub> conductance by the rice plants as a function of their tiller density.

### Soil biogeochemistry

Figure 1 provides a schematic description of the soil biogeochemistry submodels in the current and revised models. The main goal of the revision was to quantitatively track electron transfer in each reduction and oxidation process in a soil. To do so, we introduced an additional model variable to account for the concentration of H<sub>2</sub> in the soil. H<sub>2</sub> and DOC are the immediate electron donors for the series of reductive reactions (denitrification; reduction of Mn<sup>4+</sup>, Fe<sup>3+</sup>, and SO<sub>4</sub><sup>2-</sup>; and CH<sub>4</sub> production) in anaerobic soils (Lovley &

Goodwin, 1988; Achtnich *et al.*, 1995). The rates of these reactions are thus limited by the availability of H<sub>2</sub> and DOC in the soil. The revised model now calculates the production of H<sub>2</sub> and DOC from anaerobic decomposition and exudation by rice roots, and calculates the rates of reductive reactions by means of kinetic equations that depend on the concentrations of electron donors and acceptors. Following this approach, it will become possible to quantitatively predict the effects of alternative electron acceptors on CH<sub>4</sub> production. The methane emission rate is then calculated based on the conductance and density of rice tillers.

### Tests of the revised model

#### Site description

The revised DNDC was tested against datasets from rice paddy fields at two sites in Japan and one site in China: National Institute for Agro-Environmental Sciences (NIAES) (36°03'N), Kamikawa (43°51'N), and Nanjing (31°58'N). At the Japanese sites, experiments were conducted to assess the effects of rice residue management on CH<sub>4</sub> emission. At Nanjing, on the other hand, the effect of fertilizers (urea and ammonium sulfate) on CH<sub>4</sub> emission was investigated. DNDC had been previously tested at the Nanjing site, but the effect of fertilizers was not included in that validation (Cai *et al.*, 2003).

The soil properties and agricultural management at the three sites are summarized in Tables 1–4. Most of the data for Kamikawa and Nanjing were compiled from previous publications (Cai *et al.*, 1997; Goto *et al.*, 2004). Reducible soil Fe<sup>3+</sup> was measured for NIAES and Kamikawa, but no data were available for Nanjing. Thus, reducible soil Fe<sup>3+</sup> at Nanjing was provisionally set to the approximate median of reducible Fe<sup>3+</sup> of 18 soils collected from regions around the world (van Bodegom *et al.*, 2003). Reducible soil Mn<sup>4+</sup> was assumed to be 1% of the level of reducible Fe<sup>3+</sup> based on measurements from three different types of Japanese paddy soil (Hanaki *et al.*, 2002). The pool of native soil SO<sub>4</sub><sup>2-</sup> was assumed to be minimal (1 mmol kg<sup>-1</sup>) because each field used in our study was routinely fertilized with phosphate, which is selectively adsorbed on soils, where it replaces SO<sub>4</sub><sup>2-</sup> and other anions (Goldberg & Sposito, 1984; Nanzyo, 1989).

Input data to run the model included daily climatic data (maximum and minimum air temperatures, precipitation, solar radiation, and mean wind speed) at NIAES provided by a climate data acquisition station near each site. At Kamikawa, the climate data were compiled from the database of the nearest observation station of the Japan Meteorological Agency. Daily cli-

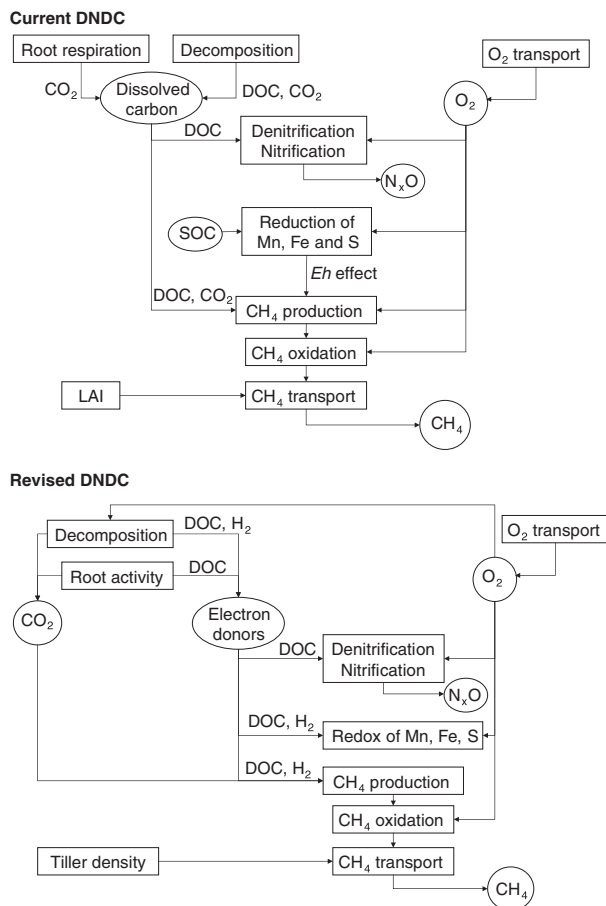


**Fig. 1** Schematic descriptions of the soil biogeochemistry submodels in the current and revised versions of DNDC (DOC, dissolved organic carbon; SOC, soil organic carbon).

mate data for Nanjing were compiled from the database of the World Meteorological Organization. Because wind speed data at Nanjing were unavailable, a default value of 0.5 ms<sup>-1</sup> was assumed for that site. A default value of daily relative humidity (70%) was used for all sites.

NIAES. At the NIAES in Tsukuba, the 'Nipponbare' rice cultivar was grown in six lysimeters (3 m × 3 m) filled with soil to a depth of 1 m. After harvesting in 1994, the six lysimeters were divided into three groups of two 'plots' to test different applications of rice residues

**Table 1** Soil properties in the three rice paddy fields used to test the DNDC model

	NIAES	Kamikawa	Nanjing
Texture	Light clay	Silty clay loam	Loamy clay
Bulk density (g cm <sup>-3</sup> )	0.8	1.3	1.1
Plow depth (cm)	10	15	10
pH	5.7	6.1	8.0
Total C (%)	1.8	1.3	1.1
Total N (%)	0.15	0.15	0.12
Reducible Fe <sup>3+</sup> (mmol kg <sup>-1</sup> )	130*	48†	15‡
Reducible Mn <sup>4+</sup> (mmol kg <sup>-1</sup> )§	1.30	0.48	0.15
SO <sub>4</sub> <sup>2-</sup> (mmol kg <sup>-1</sup> )¶	1.0	1.0	1.0

\*CH<sub>3</sub>COONa-extractable Fe<sup>2+</sup> in anaerobically incubated soil.

†AgCl<sub>3</sub>-extractable Fe<sup>2+</sup> of flooded field soil.

‡Provisional estimate.

§Assumed to equal 1% of reducible Fe<sup>3+</sup>.

¶Provisional estimate.

NIAES, National Institute for Agro-Environmental Sciences.

**Table 2** Management of the three rice paddies at the National Institute for Agro-Environmental Sciences (NIAES) site

Year	Date (month/day)	Straw	Stubble	No-residue
1994	Late September	Harvest	Harvest	Harvest
	10/21	Straw application (2.1 ton C ha <sup>-1</sup> ), tillage	No straw application, tillage	Removal of stubble, tillage
1995	4/6	Tillage	Tillage	Tillage
	4/21–9/2	Flooding	Flooding	Flooding
	4/22–9/14	Rice cultivation	Rice cultivation	Rice cultivation

**Table 3** Management of the three rice paddies at the Kamikawa site (Goto *et al.*, 2004)

Year	Date (month/day)	Straw-Oct.	Straw-May	Stubble
1996	5/21–9/26	Rice cultivation	Rice cultivation	Rice cultivation
	10/1	Straw application (1.5 ton C ha <sup>-1</sup> ), tillage	Straw application (1.5 ton C ha <sup>-1</sup> ), no tillage	No straw application, no tillage
1997	5/8	Tillage	Tillage	Tillage
	5/13–8/13	Flooding	Flooding	Flooding
	5/24–9/26	Rice cultivation	Rice cultivation	Rice cultivation
	10/2	Straw application (1.6 ton C ha <sup>-1</sup> ), tillage	Straw application (1.6 ton C ha <sup>-1</sup> ), no tillage	No straw application, no tillage
1998	5/6	Tillage	Tillage	Tillage
	5/10–8/17	Flooding	Flooding	Flooding
	5/20–9/21	Rice cultivation	Rice cultivation	Rice cultivation
	10/2	Straw application (1.5 ton C ha <sup>-1</sup> ), tillage	Straw application (1.5 ton C ha <sup>-1</sup> ), no tillage	No straw application, no tillage
1999	5/6	Tillage	Tillage	Tillage
	5/11–8/13	Flooding	Flooding	Flooding
	5/19–9/8	Rice cultivation	Rice cultivation	Rice cultivation

**Table 4** Management of the two rice paddies at the Nanjing site

Year	Date (month/day)	300U	300S
1994	5/23	Flooding started	Flooding started
	5/27	Urea (60 kg N ha <sup>-1</sup> ), P* and K† application, tillage	(NH <sub>4</sub> ) <sub>2</sub> SO <sub>4</sub> (60 kg N ha <sup>-1</sup> ), P* and K† application, tillage
	5/30	Rice transplanting	Rice transplanting
	6/7	Urea (120 kg N ha <sup>-1</sup> ) topdressing	(NH <sub>4</sub> ) <sub>2</sub> SO <sub>4</sub> (120 kg N ha <sup>-1</sup> ) topdressing
	6/20	Urea (60 kg N ha <sup>-1</sup> ) topdressing	(NH <sub>4</sub> ) <sub>2</sub> SO <sub>4</sub> (60 kg N ha <sup>-1</sup> ) topdressing
	7/18–7/25	Midseason drainage	Midseason drainage
	7/26–8/31	Intermittent flooding	Intermittent flooding
	7/29	Urea (60 kg N ha <sup>-1</sup> ) topdressing	(NH <sub>4</sub> ) <sub>2</sub> SO <sub>4</sub> (60 kg N ha <sup>-1</sup> ) topdressing
	9/1	Final drainage	Final drainage
	9/19	Harvest	Harvest

\*525 kg ha<sup>-1</sup> as superphosphate.

†75 kg ha<sup>-1</sup> as KCl.

(Table 2). In the Straw plot, rice straw equivalent to 2.1 ton C ha<sup>-1</sup> was applied to the soil, followed by tillage to incorporate the straw in the soil. Combined with the stubble remaining after harvesting (equivalent to 0.6 ton C ha<sup>-1</sup>), the soil thus received fresh rice residues equivalent to 2.7 ton C ha<sup>-1</sup>. In the Stubble plot, the soil was tilled with no straw applied but with the stubble remaining after harvesting incorporated into the soil. In the No-residue plot, rice stubble was completely removed before tillage. In the second year, rice was grown following the same management regime in these three plots, and CH<sub>4</sub> emission was measured every 4 h throughout the rice-growing season using a chamber (0.9 m × 0.9 m) system with automated opening and closure (Nishimura *et al.*, 2005).

*Kamikawa.* At the Hokkaido Prefectural Kamikawa Agricultural Experiment Station in Pippu, Goto *et al.* (2004) measured CH<sub>4</sub> emission from rice paddies planted with the 'Kirara 397' cultivar from 1997 to 1999. They studied the effects of straw application and tillage on CH<sub>4</sub> emission using three plots (Table 3). In the Straw-Oct. plot, rice straw (equivalent to 1.5–1.6 ton C ha<sup>-1</sup>) was top dressed on the field after harvesting in October, immediately followed by tillage to incorporate the straw and remaining stubble into the soil. In the Straw-May plot, the same quantity of rice straw was top dressed on the field after harvesting, but tillage was delayed until the following May. No straw was applied in the Stubble plot, but the stubble remaining after harvesting was left in place. Though the quantity of stubble was not measured, we assumed that 10% of stems and leaves (equivalent to ca. 0.5 ton C ha<sup>-1</sup>, including the roots) was left after harvesting each year, and included this amount of residues in the simulation. Researchers measured CH<sub>4</sub>

emission every 2–3 weeks using the closed chamber method, and estimated seasonal CH<sub>4</sub> emission from these values.

*Nanjing.* At the Jiangsu Academy of Agricultural Sciences in Nanjing, Cai *et al.* (1997) investigated the effect of urea and ammonium sulfate application on CH<sub>4</sub> emission using three application rates (0, 100, and 300 kg N ha<sup>-1</sup>). The rice cultivar 'Tai-fu-xuan' (the local name) was grown without applying organic matter (i.e. only the rice stubble, equivalent to ca. 0.5 ton C ha<sup>-1</sup>, left after harvesting was present), and a gas sample was collected twice per week using static chambers. In the present study, we used the data from the plots with 300 kg N ha<sup>-1</sup> applied as urea (300U) or ammonium sulfate (300S) to test the effects of fertilizer type on the DNDC model's prediction of CH<sub>4</sub> emission (Table 4).

#### *Initialization and calibration of the model*

*Initial soil organic C (SOC) composition.* The DNDC model assumes the presence of several different pools of SOC (i.e. residues, microbial biomass, humads, and humus), and the initial composition of the SOC inevitably affects the simulation results. However, in practice it is difficult to measure the SOC composition of a given soil. To determine the initial SOC composition, therefore, we made the following assumptions: (1) at the beginning of the study, the SOC pools are in a near-steady state due to the repetition of similar farming practices in previous years, and (2) the C pool in the humus is sufficiently stable that it does not change significantly over the time span simulated by the model (<100 years). Based on these assumptions, a preliminary run of DNDC was performed for a time period of about 20 years, with

constant inputs for climate and agricultural practices, to achieve a near-steady state for soil C pools. For the preliminary run, we assumed that rice straw was routinely applied at a rate of 1600–2000 kg C ha<sup>-1</sup> yr<sup>-1</sup>, following the typical local practices for rice farming. Preliminary run was started with soil total C set at the measured value, with provisional SOC composition set as 5% residues, 4% microbial biomass, 1% humads, and 90% humus. The C pools of residues, microbial biomass, and humads changed relatively fast in the first several years, but reached a near-steady state within the 20 years of the preliminary run. After such a preliminary run, resulting soil total C was within 0.2% from the measured value at each of the three sites studied.

**Field reduction factor.** To calculate the decomposition rate of C pools, DNDC uses a specific decomposition rate (*SDR*, with values shown in Table 5) for each component based on values obtained in laboratory incubations (Molina *et al.*, 1983; Gilmour *et al.*, 1985). However, these *SDR* are adjusted by a fixed reduction factor (*DRF*) to simulate the lower rates that are typically observed under field conditions. In the present study, we determined *DRF* by comparing runs of the model with the decomposition rates of rice straw during a period of 1–2 years at two rice sites (Otagawa and Tochigi) in central Japan (Mogi *et al.*, 1980; Yoshizawa & Nakayama, 1983). Between 60% and 70% of straw C decomposed within the first year, and *DRF* was calibrated as 0.6 to minimize the difference between simulated and observed straw decomposition (Fig. 2).

Previous studies (e.g. Li *et al.*, 1992) assigned a significantly lower value (0.025) to *DRF* based on comparison of model runs with measured soil respiration rates in agricultural fields. The low value of *DRF* in these studies can presumably be attributed to the initial composition of SOC that was assumed in the model simulations. Previous studies used default values for initial SOC composition (i.e. 8%, 2%, 10%, and 80% for residue, microbial biomass, humads, and

**Table 5** Specific decomposition rates (*SDRs*) for the soil C pools used in the DNDC model

Pool	Component	<i>SDR</i> (day <sup>-1</sup> )
Residue	Very labile	0.250
	Labile	0.074
	Resistant	0.020
Microbial biomass	Labile	0.330
	Resistant	0.040
Humads	Labile	0.160
	Resistant	0.006

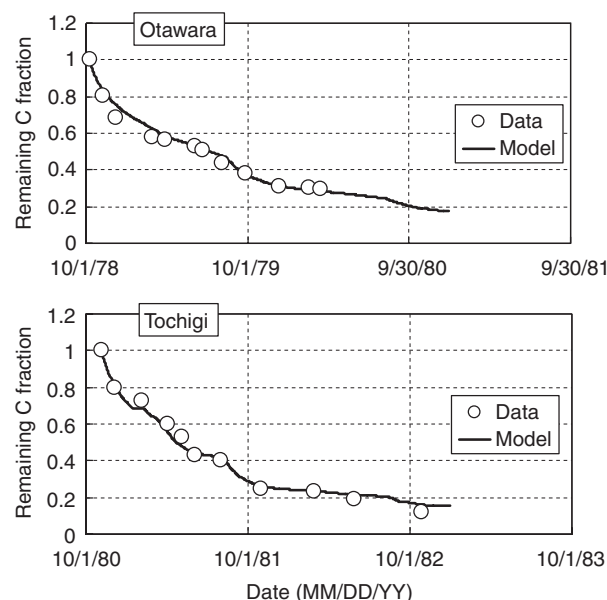


**Fig. 2** Observed and simulated straw decomposition rates at two paddy fields in Tochigi prefecture, Japan.

humus, respectively). However, this assumption may tend to overestimate the pools of decomposable SOC (residue, microbial biomass, and humads). In the present study that used *DRF* of 0.6, the initial SOC composition at NIAES site, for example, were estimated to be 5%, 2%, 4%, and 89% for residues, microbial biomass, humads, and humus, respectively. Annual soil respiration rate at the same site was estimated to be ca. 2700 kg C ha<sup>-1</sup>. If the default SOC composition was used, however, *DRF* had to be decreased to ca. 0.04 to give a comparable soil respiration rate. This example indicates that in previous studies, *DRF* was adjusted to correct for the assumption of large pools of decomposable SOC. Nevertheless, DNDC gave reasonable predictions of CH<sub>4</sub> emission from a range of rice fields (Li, 2000; Li *et al.*, 2002; Cai *et al.*, 2003; Babu *et al.*, 2006), suggesting that using an adjusted *DRF* was a practical way to simulate the CH<sub>4</sub> emission processes, at least at the studied sites. Further research may be needed to clarify the initial SOC composition of a soil and its effects on the simulation results.

**Developmental rate of rice.** Different rice cultivars were grown at the studied sites, and the growth characteristics of the different cultivars probably differed. To account for the effects of these differences, we calibrated two parameters of rice growth, the developmental rate constants at the vegetative stage (*DRCV*) and the reproductive stage (*DRCR*), for each cultivar by matching the predicted heading and maturation dates to observed values. As the actual

heading date was not clear at Nanjing, it was assumed to be early August at that site.

## Results and discussion

### Rice growth

Data were available on grain yield at harvest for all three sites, and shoot biomass (sum of stems, leaves, and panicles) at harvest for the NIAES and Kamikawa sites (The Kamikawa data were provided by E. Goto and S. Miura, Hokkaido Prefectural Kamikawa Agricultural Experiment Station). Figure 3 compares the observed and simulated values of shoot biomass and grain yield. The model tended to underestimate shoot biomass, but the relative error was  $<12\%$ . Grain yield at Kamikawa and Nanjing was predicted with a relative error of  $<13\%$ . However, grain yield at NIAES was overestimated, presumably due to alterations in canopy climate, solar radiation, and temperature in particular, because of the chambers used for  $\text{CH}_4$  measurement. In the No-residue plot at NIAES, rice growth in one replicate was abnormally decreased ( $-27\%$  in shoot biomass) compared with the other. Thus, the data from this replicate were excluded from the analysis. Even after this exclusion, the observed grain yield in the No-residue plot was obviously lower than those in the other plots, suggesting growth anomalies caused by the removal of plant residues (Fig. 3). Excluding the No-residue plot, the relative error in predicted grain yield was  $<28\%$ .

### Water temperature

Shimono (2003) provided data on flood water temperatures in the paddy fields at Kamikawa from late May or early June through mid-August in 1998 and 1999. Figure 4 presents the observed daily air and flood water temperatures, together with the predicted flood water

temperature at Kamikawa. The observed average flood water temperatures were 21.0 and 21.9 °C in 1998 and 1999, respectively, and they were 3.0 and 2.1 °C higher than the average air temperatures for the corresponding years. Because it is clear that flood water temperatures can significantly affect biogeochemical processes in flooded paddy soils, flood water temperature should be treated as a separate variable from air temperature in the model. Predicted daily flood water temperature occasionally deviated from the observed value by up to 5 °C, but the average error was within  $\pm 1.0$  °C ( $-0.95$  and 0.34 °C in 1998 and 1999, respectively) (Fig. 4).

### Methane emission and electron budgets

Figures 5–7 compare the observed and simulated daily  $\text{CH}_4$  fluxes for the three sites, and Table 6 compares the observed and simulated seasonal  $\text{CH}_4$  emissions. As a quantitative indicator of model performance on daily  $\text{CH}_4$  fluxes, Table 6 also shows root mean squared error (RMSE) of simulated daily fluxes, together with the average of both observed and simulated fluxes, in case daily flux data were available in publications. In addition to  $\text{CH}_4$  fluxes, Figures 5–7 show the calculated electron budgets for the flooded soils [i.e. the production of  $\text{H}_2$  and DOC (electron donors) as a result of organic matter decomposition and root exudation, and consumption of these electron donors by reduction of  $\text{NO}_3^-$ ,  $\text{Mn}^{4+}$ ,  $\text{Fe}^{3+}$ ,  $\text{SO}_4^{2-}$ , and C]. In this context, reduction of C is equivalent to  $\text{CH}_4$  production.

NIAES. The highest  $\text{CH}_4$  emission was observed from the Straw plot, with remarkably lower emission from the Stubble and No-residue plots (Fig. 5a, Table 6). The model's predictions were generally consistent with the observed data with respect to seasonal  $\text{CH}_4$  emission trends and magnitudes. However, daily  $\text{CH}_4$  flux was underestimated early in the rice-growing

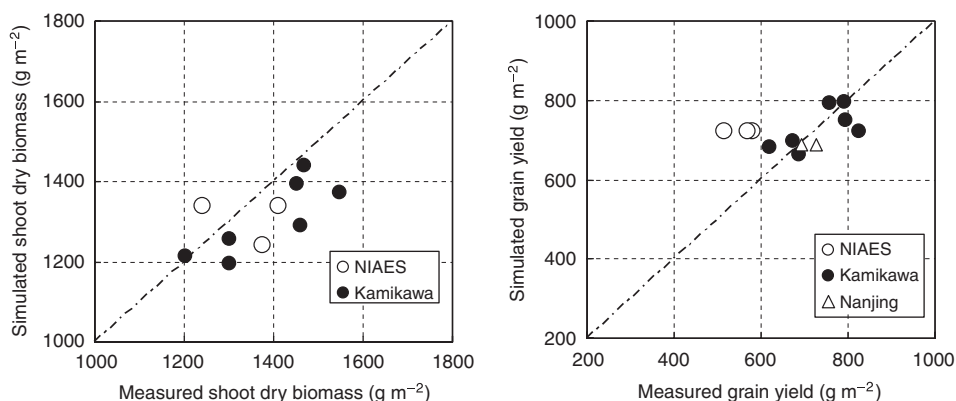
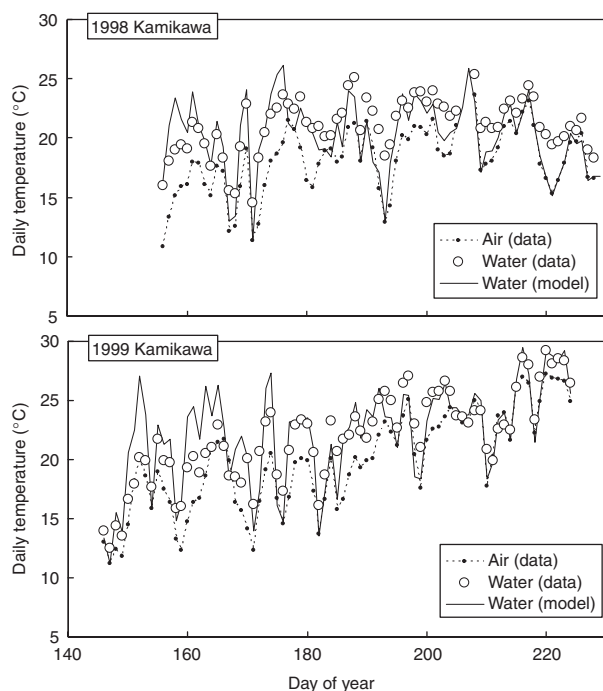


Fig. 3 Observed and simulated values of (left) shoot biomass and (right) grain yield for rice paddy fields at National Institute for Agro-Environmental Sciences (NIAES), Kamikawa, and Nanjing. Diagonal lines represent the line  $y = x$ .



**Fig. 4** Predicted flood water temperature, along with observed air and flood water temperatures, in the paddy field at Kamikawa in 1998 and 1999.

season, and was overestimated late in the growing season, particularly for the Straw plot. The RMSE of predicted daily  $\text{CH}_4$  fluxes from the Straw plot was  $0.73 \text{ kg C ha}^{-1} \text{ day}^{-1}$  for the entire observation period, though relatively large errors were made during 2 weeks after the field drainage, when a sharp peak of  $\text{CH}_4$  flux appeared (excluding the data after field drainage, the RMSE of predicted fluxes was  $0.42 \text{ kg C ha}^{-1} \text{ day}^{-1}$ ). We hypothesize the following possible explanations for these discrepancies:

First, the model assumes that paddy soils are a homogeneous system. In reality, however, the spatial distributions of the components that control  $\text{CH}_4$  production, including rice residues, Fe oxides, and rice roots, are most likely heterogeneous. Under such conditions,  $\text{CH}_4$  flux is not only temporally but also spatially variable, and observed  $\text{CH}_4$  flux is the spatial average for a certain part of the field (in case of NIAES site, the area of  $0.9 \text{ m} \times 0.9 \text{ m}$  covered by the automatic chamber). Consequently, observed  $\text{CH}_4$  flux can be different from simulations that assume homogeneous soil. To test this hypothesis, we ran the model on a hypothetical, rather simplified case of 'heterogeneous' soil system, where the soil in the Straw plot at NIAES was assumed to consist of evenly distributed regions with high, medium, and low concentrations (195, 130, and  $65 \text{ mmol kg}^{-1}$ ) of reducible  $\text{Fe}^{3+}$ . To simulate  $\text{CH}_4$  emission from such a soil system, we ran the model

separately varying the reducible  $\text{Fe}^{3+}$  concentrations at 195, 130, and  $65 \text{ mmol kg}^{-1}$ , and calculated the average of daily  $\text{CH}_4$  fluxes from these three conditions (Fig. 8). Apparently, simulated  $\text{CH}_4$  emission was substantially enhanced with low  $\text{Fe}^{3+}$  concentration, whereas repressed with high  $\text{Fe}^{3+}$  concentration (sensitivity of the model to reducible soil  $\text{Fe}^{3+}$  is discussed later in more detail). As the average of the  $\text{CH}_4$  fluxes from soil regions with different  $\text{Fe}^{3+}$  concentrations, daily  $\text{CH}_4$  fluxes from the hypothetical 'heterogeneous' soil system showed a better agreement with observation (RMSE =  $0.49 \text{ kg C ha}^{-1} \text{ day}^{-1}$ ) than the prediction assuming a homogeneous soil system (excluding the data after field drainage, the RMSE was  $0.19 \text{ kg C ha}^{-1} \text{ day}^{-1}$ ). Such an analysis, by itself alone, does not completely explain the discrepancies between observed and predicted  $\text{CH}_4$  fluxes, but nevertheless indicates that soil heterogeneity can be a cause for the discrepancies.

Second, modeling of  $\text{CH}_4$  transport processes through rice plants may be incomplete in the current model. As described in the Appendix A, this model calculates  $\text{CH}_4$  transport through rice plants based on the conductance of rice tillers, and expresses this parameter as a function of temperature and phenological stage based on fitting of data from experiments with the Japanese 'Koshihikari' cultivar. However, the rice planted at this site was 'Nipponbare,' another Japanese cultivar, and numerous studies have shown that  $\text{CH}_4$  transport characteristics can differ widely between cultivars (Yao *et al.*, 2000; Aulakh *et al.*, 2002). Prediction errors of this nature could be solved, at least partly, by introducing cultivar-specific parameters into the model.

In terms of seasonal  $\text{CH}_4$  emission, model prediction was satisfactory: the largest error was found in the No-residue plot, but it was only  $10 \text{ kg C ha}^{-1}$ . The model was thus able to predict seasonal  $\text{CH}_4$  emission and the effect of rice residue management on emissions.

The simulated electron budget (Fig. 5b) demonstrates how the model accounted for the contributions from organic matter, rice roots, and alternative electron acceptors to  $\text{CH}_4$  production in flooded soils. Rice straw application in the Straw plot obviously increased  $\text{H}_2$  production by anaerobic decomposition, and most of the increase in the  $\text{H}_2$  supply was used to support  $\text{CH}_4$  production. Straw application affected DOC production little, with root exudation being the main source of DOC. Root exudation, in turn, accounted for half or more of the electron donor supply in flooded soils. A large proportion of the electron donors were consumed to reduce  $\text{Fe}^{3+}$ , which was the strongest competitor with  $\text{CH}_4$  production for electrons.

*Kamikawa.* Observed  $\text{CH}_4$  emission from the three plots was Straw-May > Straw-Oct. > Stubble (Fig. 6a, Table 6).

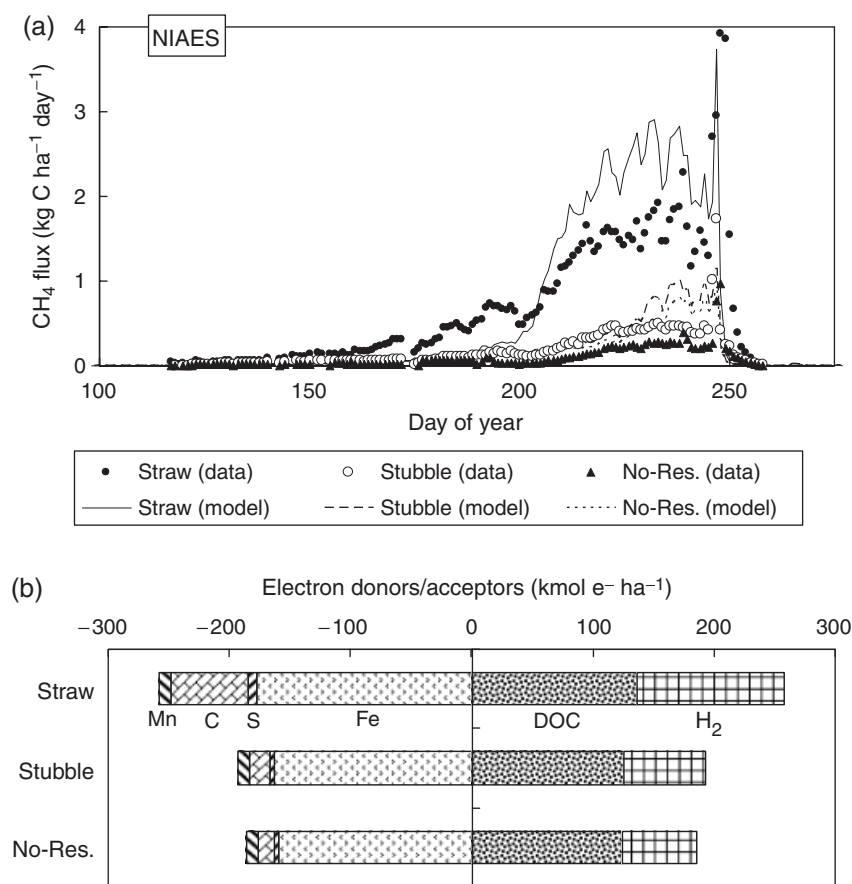


Fig. 5 (a) Observed and simulated daily methane fluxes and (b) simulated electron budgets in flooded soils for the rice paddy fields at National Institute for Agro-Environmental Sciences (NIAES).

As discussed by Goto *et al.* (2004), the lower CH<sub>4</sub> emission from the Straw-Oct. plot than in the Straw-May plot can be attributed to enhanced straw decomposition during the fallow season due to tillage in October. As was the case at NIAES, the model predictions were consistent with the observations with respect to variation in CH<sub>4</sub> emission due to rice residue management (Fig. 6a, Table 6). In the simulation, differences in rice residue management were reflected mostly in H<sub>2</sub> production by anaerobic decomposition, and consequently in CH<sub>4</sub> production in flooded soils (Fig. 6b). With respect to daily CH<sub>4</sub> flux, the model underestimated the observed values earlier in the growing season, and overestimated observed values later in the growing season (Fig. 6a), as was the case at NIAES, and the reasons for these discrepancies also appear to be similar.

With respect to seasonal CH<sub>4</sub> emission, the model's predictions were satisfactory for 1997 and 1999: the deviation from observed values was <20 kg C ha<sup>-1</sup> for each plot (Table 6). For 1998, however, the observed CH<sub>4</sub> emission from each plot was approximately half the corresponding value in the other years, and the

model overestimated the observed values. We hypothesize that this was caused, at least partly, by overestimation of rice root biomass, because the simulated root biomass for 1998 was 29–36% larger than in 1997 and 1999 at its maximum (Fig. 9). The measured shoot biomass at harvest in 1998 was greater than in the other 2 years, but the difference was <12%. To test our hypothesis, we ran another simulation in which root biomass in 1998 was decreased by 35% to a level similar to those in 1997 and 1999 (Table 7). The predicted CH<sub>4</sub> emission became much closer to the observed values, though a difference of up to 47 kg C ha<sup>-1</sup> was still apparent in the Straw-Oct. plot.

In the original simulation, the large predicted root biomass in 1998 was presumably caused by climatic conditions. During the 1998 growing season, average air temperature was relatively low (18.4, 17.1, and 18.2 °C in 1997, 1998, and 1999, respectively), but average solar radiation was relatively high (18.4, 19.7, and 18.6 MJ m<sup>-2</sup> day<sup>-1</sup>). The revised DNDC model assumes that lower temperature delays the phenological development of rice, but does not account for

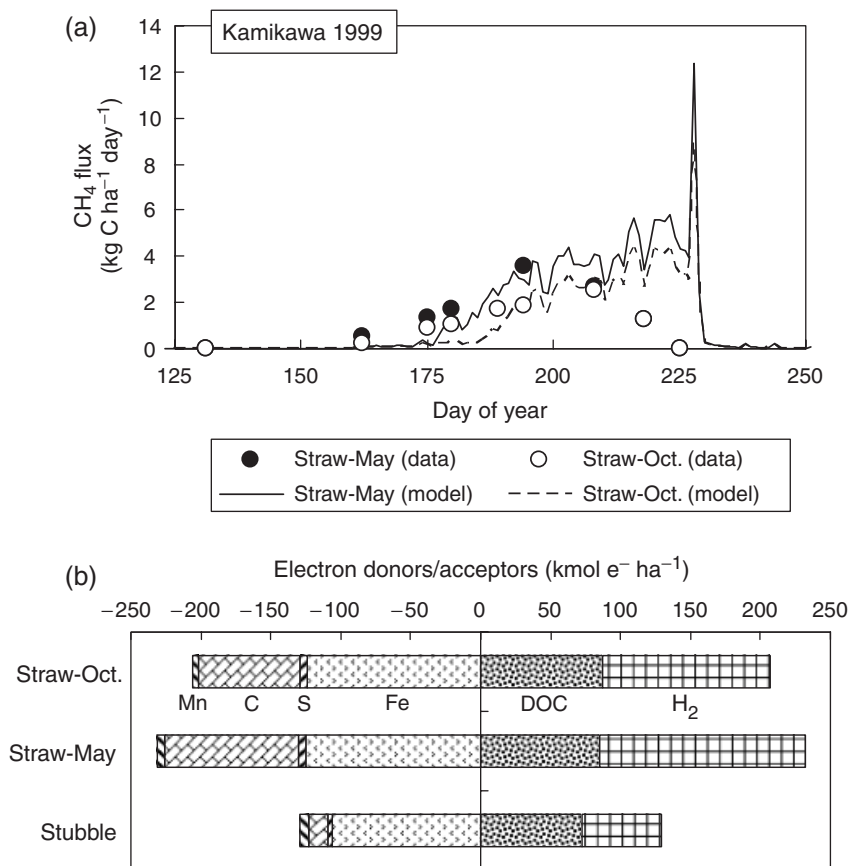


**Fig. 6** (a) Observed and simulated daily methane fluxes and (b) simulated electron budgets in flooded soils for the rice paddy fields at Kamikawa in 1999.

the direct effects of temperature on leaf area development, which is assumed to depend indirectly on solar radiation via photosynthetic C fixation and allocation to leaves. The model is also designed to allocate a greater proportion of photosynthate to roots at earlier developmental stages. Consequently, the combination of relatively low temperature and high solar radiation would have resulted in a longer vegetative growth period and increased root biomass in the simulation. Thus, the present model may have overestimated root biomass in 1998 by not accounting for the temperature dependence of leaf expansion. As rice roots are a major source of electron donors (particularly for DOC) in the paddy soils, the estimation of root biomass directly influences the prediction of CH<sub>4</sub> emission. Our results indicate that the revised DNDC still holds considerable uncertainty in estimating rice root biomass, and presumably the biomass of other organs as well, due to its inability to account for the temperature dependence of leaf area development.

*Nanjing.* This site was chosen to test the model's prediction of the effect of fertilizer type on CH<sub>4</sub>

emission. The observed CH<sub>4</sub> emission from the 300S plot was lower than that from the 300U plot (Fig. 7a, Table 6), though the difference was not statistically significant because of large variations between three replicates (Cai *et al.*, 1997). In both the 300U and 300S plots, CH<sub>4</sub> emission appears to have been decreased by intermittent irrigation later in the growing season.

Predicted CH<sub>4</sub> emission was consistent with the observation, with respect to the highest level of fluxes (ca. 1.0–2.5 kg C ha<sup>-1</sup> day<sup>-1</sup>) during continuous flooding, and the low level of fluxes (<0.5 kg C ha<sup>-1</sup> day<sup>-1</sup>) during intermittent irrigation (Fig. 7a). However, predicted daily CH<sub>4</sub> fluxes did not necessarily match the observed values, with RMSE of 0.58 and 0.32 kg C ha<sup>-1</sup> day<sup>-1</sup> for the 300U and 300S plots, respectively. As was the case at the other sites, the difference between predicted and observed CH<sub>4</sub> fluxes may have been caused by soil heterogeneity or cultivar-specific CH<sub>4</sub> transport characteristics that were not fully described by the model. In particular, reducible soil Fe was an estimated provisional value instead of measured data, and this increased the uncertainty of the predictions.

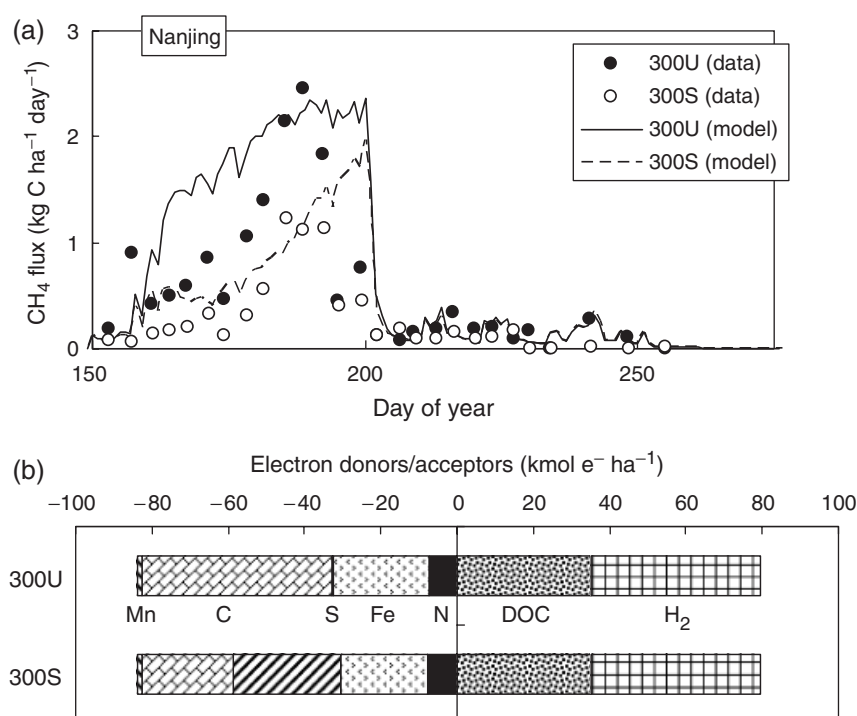


**Fig. 7** (a) Observed and simulated daily methane fluxes and (b) simulated electron budgets in flooded soils for the rice paddy fields at Nanjing.

Despite those uncertainties, the model accurately predicted the negative effect of ammonium sulfate on CH<sub>4</sub> emission (Fig. 7a, Table 6). As shown in the electron budgets (Fig. 7b), this was done by

accounting for the electron donors and competitive reduction of electron acceptors. In the simulation, reduction of S was enhanced by 28 kmol e<sup>-</sup> ha<sup>-1</sup> in the 300S plot compared with the 300N plot. The amount of

**Table 6** Comparison between observed and simulated methane (CH<sub>4</sub>) emissions during rice-growing seasons

Site	Year	Plot	Seasonal emission (kg C ha <sup>-1</sup> )		Daily flux (kg C ha <sup>-1</sup> day <sup>-1</sup> )		RMSE‡
			Obs.	Sim.	Obs.*	Sim.†	
NIAES	1995	Straw	96	97	0.71	0.72	0.73
		Stubble	25	24	0.18	0.18	0.20
		No residue	13	21	0.09	0.15	0.16
Kamikawa	1997	Straw-Oct.	80	97			
		1998	Straw-Oct.	39	102		
	1999	Straw-May	71	124			
		Stubble	11	17			
		Straw-Oct.	90	109	1.05	1.43	0.89
		Straw-May	128	143	1.40	1.88	1.17
Nanjing	1994	300U	58	88	0.59	0.87	0.58
		300S	27	47	0.27	0.48	0.32

\*Average of observed daily CH<sub>4</sub> fluxes.

†Average of simulated daily CH<sub>4</sub> fluxes on days when daily flux was measured.

‡Root mean square error of simulated daily CH<sub>4</sub> fluxes.

NIAES, National Institute for Agro-Environmental Sciences.

$\text{SO}_4^{2-}$  applied in the 300S plot was  $10.7 \text{ kmol ha}^{-1}$ , and 1 mol of  $\text{SO}_4^{2-}$  can accept 8 mol of electrons during its reduction to  $\text{H}_2\text{S}$ . Thus, the simulation indicates that 33% of the applied  $\text{SO}_4^{2-}$  was reduced in flooded soils. Previously, Li *et al.* (2004) conducted a sensitivity test on the DNDC model using alternative fertilization scenarios, in which N was applied as urea, ammonium sulfate, nitrate, or ammonium bicarbonate at a rate of  $250 \text{ kg N ha}^{-1} \text{ yr}^{-1}$ . In that test, however, fertilizer type had virtually no impact on  $\text{CH}_4$  emission.

#### Sensitivity to the reducible $\text{Fe}^{3+}$ concentration

As shown in the electron budgets in Figs 5–7,  $\text{Fe}^{3+}$  is the major competitor to  $\text{CH}_4$  production for the electron donors. Consequently, uncertainty in the concentration of reducible soil  $\text{Fe}^{3+}$  affects predictions of  $\text{CH}_4$  emission. To demonstrate the sensitivity of the model to the input value used for reducible soil  $\text{Fe}^{3+}$ , we ran the model with three levels of Fe concentration: actual measured levels, +50%, and –50% with respect to these

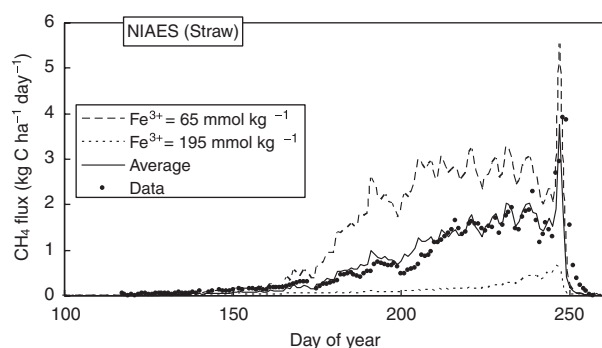


**Fig. 8** Simulated daily methane fluxes from the Straw plot at National Institute for Agro-Environmental Sciences (NIAES), assuming a hypothetical heterogeneous soil system. The soil was assumed to consist of regions with different concentrations of reducible  $\text{Fe}^{3+}$  (65, 130, and  $195 \text{ mmol kg}^{-1}$ ), and the solid line represents the average of daily methane fluxes from those regions. Simulated methane flux assuming reducible  $\text{Fe}^{3+}$  of  $130 \text{ mmol kg}^{-1}$  is shown in Fig. 5a.

levels. Table 8 shows the effect of reducible soil  $\text{Fe}^{3+}$  on simulated  $\text{CH}_4$  emissions at the NIAES and Kamikawa sites (daily  $\text{CH}_4$  fluxes from NIAES site with  $\pm 50\%$   $\text{Fe}^{3+}$  are shown in Fig. 8). When  $\text{Fe}^{3+}$  was decreased by 50%, simulated  $\text{CH}_4$  emission was substantially increased at each site (+88% at NIAES, +66% at Kamikawa). In contrast, when the  $\text{Fe}^{3+}$  concentration was increased by 50%, simulated  $\text{CH}_4$  emission was decreased by 85% and 40% at NIAES and Kamikawa, respectively. These results clearly indicate that the model is highly sensitive to the reducible  $\text{Fe}^{3+}$  concentration, and that consequently, this parameter must be estimated correctly to permit reliable prediction of  $\text{CH}_4$  emissions. When considering regional application of the model, however, it would be impractical to determine reducible soil  $\text{Fe}^{3+}$  by means of laboratory incubation or field measurements at a regional scale. Van Bodegom *et al.* (2003) proposed a solution based on regression equations for predicting reducible  $\text{Fe}^{3+}$  from data on oxalate-extractable Fe and dithionite citrate-extractable Fe. Using such equations in combination with a soil database may permit more accurate estimation of reducible soil  $\text{Fe}^{3+}$  at a regional scale.

#### Uncertainty in plant parameters

Because the growth characteristics of rice vary widely among cultivars, at least two parameters in the model must be determined for each cultivar. In the present study, we tested the effects of incorporating phenological development rates in the vegetative and reproductive stages on the model's predictive ability. We chose these parameters because it should not be very difficult to obtain information on typical heading and maturation dates for the dominant cultivars in specific regions. Other important parameters are carbon allocation to root biomass, as well as the conductance of rice tillers for  $\text{CH}_4$  transport. As suggested by the Kamikawa simulation, the model still holds considerable uncertainty in estimating rice root biomass, and this uncertainty can strongly affect the predicted  $\text{CH}_4$  production.

**Table 7** Effect of root biomass on simulated seasonal methane ( $\text{CH}_4$ ) emissions from the Kamikawa paddy fields

Site	Year	Plot	Observed emission ( $\text{kg C ha}^{-1}$ )	Simulated emission ( $\text{kg C ha}^{-1}$ )	
				a	b
Kamikawa	1998	Straw-Oct.	39	102	86
		Straw-May	71	124	98
		Stubble	11	17	10

Maximum root dry biomass was approximately (a)  $840 \text{ kg ha}^{-1}$  or (b)  $550 \text{ kg ha}^{-1}$ .

The model's simulation of CH<sub>4</sub> emission through rice plants uses a diffusion model based on the tiller conductance determined for 'Koshihikari.' However, Yao *et al.* (2000) measured the conductance of 11 cultivars (nine from Japan, one from the United States, and one from the International Rice Research Institute in the Philippines), and showed that the conductance varied significantly among cultivars. Therefore, variations in conductance among cultivars could be a source of additional uncertainty. Note, however, that the revised DNDC described in the present paper can address the issue of varietal differences in CH<sub>4</sub> emission due to differences in conductance if this parameter can be determined for each cultivar; in contrast, the current DNDC model lacks such a capability.

#### Advantages of the revised DNDC model over current models

**Soil climate.** In current versions of DNDC, the soil temperature profile is calculated using a heat flux model, which assumes that the soil surface temperature equals the daily average air temperature. However, Shimono *et al.* (2002) and Shimono (2003) have demonstrated that the flood water of paddy fields can be substantially warmer than the atmosphere (by 5 °C or more) because of the water's ability to absorb solar radiation, and the difference between water and air temperatures is generally larger in cooler climates. Thus, the current DNDC is likely to underestimate the temperature of flooded

paddy soils, particularly under cooler conditions. By incorporating a micrometeorological model, the revised DNDC can estimate daily flood water temperatures (Fig. 4), thereby improving the estimation of soil temperature profiles.

**Anaerobic soil processes.** A number of process-based or semiempirical models have been proposed, including current versions of DNDC, that are capable of simulating CH<sub>4</sub> emissions from rice paddy fields or natural wetlands at the ecosystem scale (e.g. Cao *et al.*, 1995; Walter *et al.*, 1996; Huang *et al.*, 1998; Li, 2000; Walter & Heimann, 2000; Li *et al.*, 2004). These models calculate CH<sub>4</sub> production based on the C supply from the soil and plant, using soil *Eh* as an environmental factor that regulates CH<sub>4</sub> production. However, as these models do not quantify electron donors and acceptors in their calculation of soil *Eh*, they cannot account for the effects of changes in the quantities and proportions of electron acceptors on CH<sub>4</sub> production under various conditions. These models assume already-reduced conditions (Cao *et al.*, 1995; Walter *et al.*, 1996; Walter & Heimann, 2000), or estimate soil *Eh* as an empirical function of flooding duration (Huang *et al.*, 1998). Current versions of DNDC (e.g. Li *et al.*, 2004) link soil *Eh* to oxidant reduction by combining the following equations:

$$F_{\text{oxidant}} = a \left( \frac{[\text{DOC}]}{b + [\text{DOC}]} \right) \left( \frac{[\text{oxidant}]}{c + [\text{oxidant}]} \right), \quad (1)$$

$$Eh = E_0 + \frac{RT}{nF} \ln \frac{[\text{oxidant}]}{[\text{reductant}]}, \quad (2)$$

where  $F_{\text{oxidant}}$  is the fraction of the oxidant that is reduced during a given time step, square brackets represent concentration values, and  $a$ ,  $b$ , and  $c$  are coefficients. Although Eqn (1) relates the oxidant reduction rate to the concentrations of DOC and oxidants, the current DNDC does not account for the consumption of electron donors by oxidant reduction. Consequently, soil *Eh* is not influenced by the initial concentration of oxidants. For example, we tested the sensitivity of version 8.2L of DNDC to the reducible Fe<sup>3+</sup> concentration, using data from the NIAES Straw

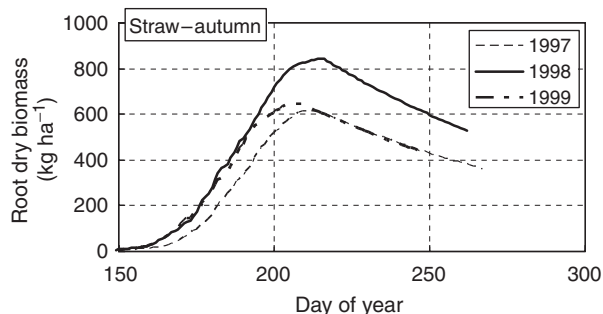


Fig. 9 Simulated root biomass in the Straw-Oct. plot of the Kamikawa rice paddy fields from 1997 to 1999.

Table 8 Effects of the concentration of reducible soil Fe<sup>3+</sup> on simulated seasonal methane (CH<sub>4</sub>) emission from paddy fields

Site	Year	Plot	Observed emission (kg C ha <sup>-1</sup> )	Simulated emission (kg C ha <sup>-1</sup> )		
				-50% Fe	Actual Fe	+50% Fe
NIAES	1995	Straw	96	182	97	15
Kamikawa	1999	Straw-Oct.	90	181	109	65

NIAES, National Institute for Agro-Environmental Sciences.

plot. In contrast to the revised model, reducible  $\text{Fe}^{3+}$  concentration in version 8.2L of the model did not affect soil  $Eh$  and  $\text{CH}_4$  emission, which was calculated as  $176 \text{ kg C ha}^{-1} \text{ yr}^{-1}$  for all  $\text{Fe}^{3+}$  concentrations.

In contrast, the revised DNDC model presented in this study quantifies production and consumption of electron donors in relevant soil processes. By adopting such an approach, the progress of reductive reactions ( $\text{CH}_4$  production and the reduction of electron acceptors) is explicitly limited by the supply of electron donors from decomposition of SOC and from root exudation. Consequently, it is possible to quantitatively assess the effects of electron acceptors on  $\text{CH}_4$  production. The revised model also simulates  $\text{CH}_4$  emission through rice plants based on the conductance and density of rice tillers. Thus, it will be capable of assessing the impacts of climate and agricultural management on  $\text{CH}_4$  emission by their effects on the conductance or density of rice tillers.

*Crop growth.* The current DNDC calculates crop N uptake based on accumulated temperature, and calculates crop growth based on the N uptake, subject to water or N stress. This approach is convenient because it allows the simulation of various crops using relatively simple algorithms, but cannot account explicitly for the effects of climate and agronomic management on crop growth, and the resultant changes in soil C metabolism, including  $\text{CH}_4$  generation and emission through rice plants.

#### *Implications of our results for previous studies with DNDC model*

In previous studies (Li *et al.*, 2002, 2005, 2006), DNDC was applied to study rice agriculture in China at the national scale to estimate GHG ( $\text{CH}_4$ ,  $\text{CO}_2$ , and  $\text{N}_2\text{O}$ ) emissions and the impact of mitigation options, including alternative forms of water management and fertilizer application. Prior to this national-scale application, DNDC was validated against site-scale datasets for  $\text{CH}_4$  emission from rice fields in several countries (Li *et al.*, 2002; Cai *et al.*, 2003). In those studies, DNDC estimated  $\text{CH}_4$  production ( $PRD_{\text{CH}_4}$ ) based on the C supply from the soil and rice plants using empirical coefficients and factors in the following formula:

$$PRD_{\text{CH}_4} = (k_1[\text{CO}_2] + k_2[\text{DOC}])f_T f_{Eh} f_{pH}, \quad (3)$$

where  $[\text{CO}_2]$  and  $[\text{DOC}]$  are the concentrations of  $\text{CO}_2$  and DOC in the soil;  $k_1$  and  $k_2$  are rate coefficients; and  $f_T$ ,  $f_{Eh}$ , and  $f_{pH}$  are factors describing the effects of soil temperature,  $Eh$ , and pH, respectively.

In the validation cases, DNDC showed acceptable agreement with most observations, indicating that the

coefficients and factors used in the model had been determined appropriately to provide good estimates of  $\text{CH}_4$  emission. However, as mentioned earlier, the current DNDC does not respond to variations in the contents of electron acceptors in soils; in the national-scale applications, in fact, soil  $\text{Fe}^{3+}$ ,  $\text{Mn}^{4+}$ , and  $\text{SO}_4^{2-}$  contents were set to estimated national averages for Chinese paddy soils. Thus, the  $\text{CH}_4$  emission estimates at a national scale did not account for the effects of variations in the contents of electron acceptors. In reality, the contents of electron acceptors will strongly affect  $\text{CH}_4$  emissions from rice fields, particularly under alternative forms of water management: draining flood water introduces atmospheric  $\text{O}_2$  into the soil and oxidizes the reduced electron acceptors, which then function once again as electron acceptors and inhibit  $\text{CH}_4$  production in subsequent flooded periods. Consequently, the impact of this alternative form of water management on  $\text{CH}_4$  emissions should be greater in soils with higher contents of electron acceptors.

In the national-scale emission estimates for China (Li *et al.*, 2005, 2006), the uncertainty of the estimates was quantified using the most-sensitive-factor (MSF) method. In the MSF method, soil texture and SOC were chosen as the most sensitive environmental factors for determining  $\text{CH}_4$  emission, and the range of  $\text{CH}_4$  emission was estimated by varying the soil texture and SOC over the range of values for these parameters reported in Chinese soil databases. However, if this analysis had also considered the variation in the soil contents of electron acceptors, the uncertainty in the emission estimates would be wider than the previously reported values. At present, however, quantitative estimation of this component of the model's uncertainty is not possible due to a lack of information on the spatial distribution of soil contents of electron acceptors. Based on the strong sensitivity of model estimates to factors such as reducible  $\text{Fe}^{3+}$  in the soil, such work is an important subject for future studies.

In this study, the model was run with constant inputs of climate and farming managements for about 20 years in the beginning, in order to achieve near-steady state in SOC pools before the simulation years. This technique is often referred to as *spin-up run* of the model, and is applied in order to reduce the effects on simulation result from uncertainties in the initial conditions, such as the composition of SOC. In previous studies on national scale applications of DNDC (Li *et al.*, 2002, 2005, 2006), however, no spin-up run was applied, starting the simulation with a fixed default SOC composition. Actually, the default composition was chosen to represent near-steady state in SOC pools, based on test runs for about 100 years on a number of separate sites. However, as steady state SOC composition will

vary depending on soil condition, climate, and farming practices, a fixed default would not apply to every site. Therefore, the use of a fixed default of SOC composition, in stead of spin-up runs, would add further uncertainties to the previous national scale estimates. Such uncertainties may become visible in the dynamics of simulation results as of Li *et al.* (2006), in which GHG emissions from rice fields in China were predicted for the period of 20 years (2001–2020) with eight management scenarios concerning water, fertilizer, and straw application. In the simulation with *baseline* scenario, for example, nationally averaged CO<sub>2</sub> emission rate from rice fields decreased monotonously in the first 8 years, from  $-350 \text{ kg C ha}^{-1} \text{ yr}^{-1}$  in 2001 to ca.  $-800 \text{ kg C ha}^{-1} \text{ yr}^{-1}$  in 2008, despite C input to soil was increased every year by raising the incorporation rate of above-ground biomass from 15% in 2001 to 50% in 2008. Then, CO<sub>2</sub> emission rate turned to increase from 2008 and reached near-steady state around  $-500 \text{ kg C ha}^{-1} \text{ yr}^{-1}$  by 2020, as the incorporation rate of above-ground biomass was fixed at 50%. Such a trend in simulated CO<sub>2</sub> emission rate was common for all the eight management scenarios, which assumed the same incorporation rate of above-ground biomass. Apparently, the continuous decrease in CO<sub>2</sub> emission rate in beginning years was due to decrease in decomposable SOC pools, which depended on the initial SOC composition. Therefore, simulated CO<sub>2</sub> emission rates in the beginning years should be regarded as under the effects of initial SOC composition, not representing the dynamics of CO<sub>2</sub> emission rate during those years. Nevertheless, as emission rates reached near-steady state by 2020 with all the management scenarios, we can judge that the simulation was free of the effects of initial SOC composition by that time, and the results in near-steady state would provide insights into the effects of mitigation options on GHG emission rate.

### Acknowledgements

The authors extend great thanks to Eiji Goto and Shu Miura, Hokkaido Prefectural Kamikawa Agricultural Experiment Station, for kindly providing the data on rice growth at the Kamikawa site. This study was financially supported in part by the Global Environment Research Coordination System, Ministry of the Environment, Japan. The involvement of Changsheng Li in this study was supported by NASA's Terrestrial Ecology project 'Atmospheric impacts of rice agriculture in Asia' (NNG05GH80G).

### References

- Acht nich C, Bak F, Conrad R (1995) Competition for electron donors among nitrate reducers, ferric iron reducers, sulfate reducers, and methanogens in anoxic paddy soil. *Biology and Fertility of Soils*, **19**, 65–72.
- Aulakh MS, Wassmann R, Rennenberg H (2002) Methane transport capacity of twenty-two rice cultivars from five major Asian rice-growing countries. *Agriculture, Ecosystems and Environment*, **91**, 59–71.
- Babu YJ, Li C, Frolking S, Nayak DR, Adhya TK (2006) Field validation of DNDC model for methane and nitrous oxide emissions from rice-based production systems in India. *Nutrient Cycling in Agroecosystems*, **74**, 157–174.
- Butterbach-Bahl K, Papen H, Rennenberg H (1997) Impact of gas transport through rice cultivars on methane emission from paddy fields. *Plant, Cell and Environment*, **20**, 1175–1183.
- Cai Z, Sawamoto T, Li C *et al.* (2003) Field validation of the DNDC model for greenhouse gas emissions in East Asia cropping systems. *Global Biogeochemical Cycles*, **17**, 1107.
- Cai Z, Xing G, Yan X, Xu H, Tsuruta H, Yagi K, Minami K (1997) Methane and nitrous oxide emissions from rice paddy fields as affected by nitrogen fertilizers and water management. *Plant and Soil*, **196**, 7–14.
- Cao M, Dent JB, Heal OW (1995) Modeling methane emissions from rice paddies. *Global Biogeochemical Cycles*, **9**, 183–195.
- Gilmour JT, Clark MD, Sigua GC (1985) Estimating net nitrogen mineralization from carbon dioxide evolution. *Soil Science Society of America Journal*, **49**, 1398–1402.
- Goldberg S, Sposito G (1984) A chemical model of phosphate adsorption by soils: I. Reference oxide minerals. *Soil Science Society of America Journal*, **48**, 772–778.
- Goto E, Miyamori Y, Hasegawa S, Inatsu O (2004) Reduction effects of accelerating rice straw decomposition and water management on methane emission from paddy fields in a cold district. *Japanese Journal of Soil Science and Plant Nutrition*, **75**, 191–201 (in Japanese with English summary).
- Gotoh S, Yamashita K (1966) Oxidation–reduction potential of a paddy soil *in situ* with special reference to the production of ferrous iron, manganous manganese and sulfide. *Soil Science and Plant Nutrition*, **12**, 230–238.
- Goudriaan J, Unsworth MH (1990) Implications of increasing carbon dioxide and climate change for agricultural productivity and water resources. In: *Impact of Carbon Dioxide, Trace Gases, and Climate Change on Global Agriculture* (eds Kimball BA, Rosenberg NJ, Allen LH Jr), pp. 111–130. American Society of Agronomy, Madison, WI.
- Hanaki M, Ito T, Saigusa M (2002) Effect of no-tillage rice (*Oryza sativa* L.) cultivation on methane emission in three paddy fields of different soil types with rice straw application. *Japanese Journal of Soil Science and Plant Nutrition*, **73**, 135–143 (in Japanese with English summary).
- Hasegawa T, Horie T (1996) Leaf nitrogen, plant age and crop dry matter production in rice. *Field Crops Research*, **47**, 107–116.
- Hosono T, Nouchi I (1997) The dependence of methane transport in rice plants on the root zone temperature. *Plant and Soil*, **191**, 233–240.
- Huang Y, Sass RS, Fisher FM Jr (1998) A semi-empirical model of methane emission from flooded rice paddy soils. *Global Change Biology*, **4**, 247–268.

- Inubushi K, Cheng W, Aonuma S *et al.* (2003) Effect of free-air CO<sub>2</sub> enrichment (FACE) on CH<sub>4</sub> emission from a rice paddy field. *Global Change Biology*, **9**, 1458–1464.
- IPCC (1995) *Climate Change 1995: Impacts, Adaptations and Mitigation of Climate Change: Scientific-Technical Analyses, Contribution of Working Group II to the Second Assessment Report of the IPCC*. WMO/UNEP, Geneva, pp. 745–771.
- Kludze HK, DeLaune RD, Patrik WH (1993) Aerenchyma formation and methane and oxygen exchange in rice. *Soil Science Society of America Journal*, **57**, 386–391.
- Kropff MJ, Van Laar HH, Matthews RB (1994) *ORYZA1: An Ecophysiological Model for Irrigated Rice Production*. SARP Research Proceedings. DLO-Research Institute for Agrobiological and Soil Fertility/WAU-Department of Theoretical Production Ecology/International Rice Research Institute, Wageningen/Wageningen/Los Baños, Philippines.
- Kuwagata T, Hamasaki T (2000) Study on the characteristics of rice paddy water temperature and its relation to dew formation on leaves. In: *Preprint Volume of the 24th Conference on Agricultural and Forest Meteorology*, pp. 133–134. American Meteorological Society, Boston.
- Lashof DA, Ahuja DR (1990) Relative contributions of greenhouse gas emissions to global warming. *Nature*, **344**, 529–531.
- Lelieveld J, Crutzen PJ, Dentener FJ (1998) Changing concentration, lifetime and climate forcing of atmospheric methane. *Tellus Series B*, **50B**, 128–150.
- Li C (2000) Modeling trace gas emissions from agricultural ecosystems. *Nutrient Cycling in Agroecosystems*, **58**, 259–276.
- Li C, Frolking S, Frolking TA (1992) A model of nitrous oxide evolution from soil driven by rainfall events: 1. Model structure and sensitivity. *Journal of Geophysical Research*, **97**, 9759–9776.
- Li C, Frolking S, Harriss R (1994) Modeling carbon biogeochemistry in agricultural soils. *Global Biogeochemical Cycles*, **8**, 237–254.
- Li C, Frolking S, Xiao X *et al.* (2005) Modeling impacts of farming management alternatives on CO<sub>2</sub>, CH<sub>4</sub>, and N<sub>2</sub>O emissions: a case study for water management of rice agriculture of China. *Global Biogeochemical Cycles*, **19**, GB3010, doi: 10.1029/2004GB002341.
- Li C, Mosier A, Wassmann R *et al.* (2004) Modeling greenhouse gas emissions from rice-based production systems: sensitivity and upscaling. *Global Biogeochemical Cycles*, **18**, GB1043, doi: 10.1019/2003GB002045.
- Li C, Qiu J, Frolking S *et al.* (2002) Reduced methane emissions from large-scale changes in water management of China's rice paddies during 1980–2000. *Geophysical Research Letters*, **29**, 1972.
- Li C, Salas W, DeAngelo B, Rose S (2006) Assessing alternatives for mitigating net greenhouse gas emissions and increasing yields from rice production in China over the next twenty years. *Journal of Environmental Quality*, **35**, 1554–1565.
- Lovley DR, Goodwin S (1988) Hydrogen concentrations as an indicator of the predominant terminal electron-accepting reactions in aquatic sediments. *Geochimica et Cosmochimica Acta*, **52**, 2993–3003.
- Mogi S, Yoshizawa T, Nakano M (1980) Studies on soil science and fertilizer in the paddy field applied rice and barley straw. (II) Decomposition process of rice straw in paddy field and changes in its chemical composition. *Bulletin of Tohigi Agricultural Experiment Station*, **26**, 17–26 (in Japanese with English summary).
- Molina JAE, Clapp CE, Shaffer MJ, Chichester FW, Larson WE (1983) NCSOIL, a model of nitrogen and carbon transformations in soil: description, calibration, and behavior. *Soil Science Society of America Journal*, **47**, 85–91.
- Nanzyo M (1989) Chemisorption of phosphate on soils and soil constituents. *Bulletin of National Institute of Agro-Environmental Sciences*, **6**, 19–73 (in Japanese with English summary).
- Nishimura S, Sudo S, Akiyama H, Yonemura S, Yagi K, Tsuruta H (2005) Development of a system for simultaneous and continuous measurement of carbon dioxide, methane and nitrous oxide fluxes from crop fields based on the automated closed chamber method. *Soil Science and Plant Nutrition*, **51**, 557–564.
- Penning de Vries FWT, Jansen DM, Ten Berge HFM, Bakema A (1989) *Simulation of Ecophysiological Processes of Growth in Several Annual Crops*. Pudoc/IRRI, Wageningen/Los Baños, 271pp.
- Schütz H, Schröder P, Rennenberg H (1991) Role of plants in regulating the methane flux to the atmosphere. In: *Trace Gas Emissions by Plants* (eds Sharkey TD, Holland EA, Mooney HA), pp. 29–63. Academic Press, San Diego.
- Shimono H (2003) *Quantitative evaluation of the effects of water temperature on rice growth and yield under cool climates*. PhD thesis, Graduate School of Agriculture, Hokkaido University, Sapporo.
- Shimono H, Hasegawa T, Iwama K (2002) Response of growth and grain yield to cool water at different growth stages in paddy rice. *Field Crops Research*, **73**, 67–79.
- Sinclair TR, Horie T (1989) Leaf nitrogen, photosynthesis, and crop radiation use efficiency: a review. *Crop Science*, **29**, 90–98.
- Takai Y (1961a) Suiden no kangen to biseibutsu taisha (Reduction of rice paddy fields and microbial metabolism). *Nougyou Gijutsu*, **16**, 1–4 (in Japanese).
- Takai Y (1961b) Suiden no kangen to biseibutsu taisha (Reduction of rice paddy fields and microbial metabolism). *Nougyou Gijutsu*, **16**, 51–53 (in Japanese).
- Takai Y (1961c) Suiden no kangen to biseibutsu taisha (Reduction of rice paddy fields and microbial metabolism). *Nougyou Gijutsu*, **16**, 122–126 (in Japanese).
- Takai Y, Koyama T, Kamura T (1957) Microbial metabolism of paddy soils. Part III. *Nippon Noeikagaku Kaishi*, **31**, 211–215 (in Japanese with English summary).
- Van Bodegom PM, Scholten JCM (2001) Microbial processes of CH<sub>4</sub> production in a rice paddy soil: model and experimental validation. *Geochimica et Cosmochimica Acta*, **65**, 2055–2066.
- Van Bodegom PM, Stams AJM (1999) Effects of alternative electron acceptors and temperature on methanogenesis in rice paddy soils. *Chemosphere*, **39**, 167–182.
- Van Bodegom PM, Van Reeven J, Denier Van Der Gon HAC (2003) Prediction of reducible soil iron from iron extraction data. *Biogeochemistry*, **64**, 231–245.
- Walter BP, Heimann M (2000) A process-based, climate-sensitive model to derive methane emissions from natural wetlands: application to five wetland sites, sensitivity to model para-

- meters, and climate. *Global Biogeochemical Cycles*, **14**, 745–765.
- Walter BP, Heimann M, Shannon RD, White JR (1996) A process-based model to derive methane emissions from natural wetlands. *Geophysical Research Letters*, **23**, 3731–3734.
- Wang B, Adachi K (2000) Differences among rice cultivars in root exudation, methane oxidation, and populations of methanogenic and methanotrophic bacteria in relation to methane emission. *Nutrient Cycling in Agroecosystems*, **58**, 349–356.
- Watson A, Stephen KD, Nedwell DB, Arah JRM (1997) Oxidation of methane in peat: kinetics of CH<sub>4</sub> and O<sub>2</sub> removal and the role of plant roots. *Soil Biology and Biochemistry*, **29**, 1257–1267.
- Yao H, Yagi K, Nouchi I (2000) Importance of physical plant properties on methane transport through several rice cultivars. *Plant and Soil*, **222**, 83–93.
- Yoshizawa T, Nakayama K (1983) Studies on soil science and fertilizer in the paddy field applied rice and barley straw. (V) Decomposition process of barley and rice straw in the paddy field and changes of soil science by application of organic matter. *Bulletin of Tohigi Agricultural Experiment Station*, **29**, 49–60 (in Japanese with English summary).
- Zhang Y, Li C, Trettin CC, Li H, Sun G (2002) An integrated model of soil, hydrology, and vegetation for carbon dynamics in wetland ecosystems. *Global Biogeochemical Cycles*, **16**, 1061.

## Appendix A: description of the revised DNDC model

The revised model described in the present paper incorporates revisions in each of the model's soil climate, crop growth, and biogeochemistry submodels.

### Soil climate submodel

We integrated a micrometeorological model (Kuwagata & Hamasaki, 2000) to allow us to estimate the daily mean temperature of the flood water in order to account for the fact that flood water can be substantially warmer than surface air as a result of its absorption of solar radiation. Based on air temperature, solar radiation, wind speed, and relative humidity, this model first calculates the temperature of nonvegetated static water by solving heat-balance equations. Then, it estimates the effects of wind speed and leaf area index on water temperature using experimental functions. To perform these calculations, the revised DNDC model uses additional site-specific data for daily mean wind speed and air relative humidity. Given the flood water temperature, the temperature of the soil profile is then calculated using the algorithms for thermal conductivity that are already present in the current DNDC model.

### Crop growth submodel

The major functions for rice growth used in the crop growth submodel are summarized in Table A1. To explicitly describe photosynthesis, respiration, and C allocation in crops, the MACROS model (Penning de Vries *et al.*, 1989) was converted into the C++ programming language so that it could be integrated into DNDC. In MACROS, direct and diffuse light are considered separately to calculate leaf photosynthetic rate, which is integrated across time and canopy layers to calculate daily canopy photosynthesis. Net carbon gain of the canopy is calculated by subtracting the respira-

tion requirement from canopy photosynthesis based on the coefficients for maintenance respiration adopted from the ORYZA1 rice model (Kropff *et al.*, 1994). The effect of N availability on leaf photosynthesis is considered using the relationship between leaf N concentration and the potential maximum photosynthetic rate proposed by Sinclair & Horie (1989). The effect of atmospheric CO<sub>2</sub> concentration on the photosynthetic rate is estimated with the  $\beta$  factor approach of Goudriaan & Unsworth (1990).

The assimilated carbon is allocated among plant organs using partitioning coefficients, which are defined as functions of the developmental stage (*DS*). Whereas the carbon partitioning in MACROS is based on table functions, the revised DNDC model uses polynomial functions derived from published data for rice (Hasegawa & Horie, 1996; Shimono *et al.*, 2002; Inubushi *et al.*, 2003). Different sets of parameters of the functions can be used for each cultivar of interest.

Leaf area increment is based on the increase in leaf weight and specific leaf area, which are defined as a function of *DS*. Loss of leaf area is calculated from the weight of the green leaves multiplied by the relative rate of leaf death (thus, weight loss), which is a function of *DS*.

*DS* is defined as 0.3, 1.0, and 2.0 at the transplanting, heading, and maturation stages, respectively, and the rate of development is calculated as a function of temperature. Because the revised DNDC uses rice tiller density to calculate CH<sub>4</sub> transportation conductance, tiller density is estimated using the heat unit model (Shimono, 2003) based on flood water temperature and initial tiller density.

To calculate the organic C supply from rice roots, it is assumed that 1% of root biomass is lost daily to the soil after the heading stage, and that root exudation occurs in direct proportion to root weight at all phenological stages. The root turnover rate is arbitrary, whereas the root exudation rate is based on laboratory measure-

**Table A1** Major functions used in the revised DNDC model for rice growth in the crop growth submodel

Function	Equation
Photosynthetic rate	$PLMXP_a = \frac{5}{1 + \exp(-4N_L + 0.8)} - 2.5 \quad (A1)$
	$F_{CO_2} = 1 + 0.4 \log \frac{[CO_2]_A}{350} \quad (A2)$
Phenological development	$DS = \begin{cases} 0.3 + \sum_{\text{days}} DRV (DS < 1.0) \\ 1.0 + \sum_{\text{days}} DRR (DS \geq 1.0) \end{cases} \quad (A3)$
	$DRV = DRCV(3 \times 10^{-5}T_A^3 - 0.0042T_A^2 + 0.1819T_A - 1.3333) \quad (A4)$
	$DRR = DRCR(-2 \times 10^{-5}T_A^3 + 6 \times 10^{-4}T_A^2 + 0.0268T_A + 0.1342) \quad (A5)$
C allocation to aboveground biomass	$CASST = \min(1, 0.8 - 0.0616DS + 0.34DS^2 - 0.0722DS^3) \quad (A6)$
C allocation to leaves 'Nipponbare' 'Kirara 397'	$CALVT = \begin{cases} 0.48 (DS < 0.45) \\ \max(0, 0.0818 + 1.78DS - 2DS^2) (0.45 \leq DS \leq 2.0) \end{cases} \quad (A7)$
	$CALVT = \begin{cases} 0.57 (DS < 0.33) \\ \max(0, 0.374 + 1.18DS - 1.78DS^2) (0.33 \leq DS \leq 2.0) \end{cases} \quad (A8)$
C allocation to stem	$CASTT = \begin{cases} 1 - CALVT (DS \leq 1.0) \\ 0 (1.0 < DS \leq 2.0) \end{cases} \quad (A9)$
Rice root exudation	$EXD = 5.87 DW_{\text{root}} \quad (A10)$
Root litter	$RTL = 0.01 BM_{\text{root}} \quad (A11)$
O <sub>2</sub> release from roots	See Fig. A1
Rice tiller density	$N_{\text{tiller}} = \begin{cases} N_{\text{tiller}}^0 \max(1, 4.45 \log(HUT) - 18.3) (HUT > 0) \\ N_{\text{tiller}}^0 (HUT \leq 0) \end{cases} \quad (A12)$
	$HUT = \sum_{\text{days}} \max(0, T_W - 15) (DS < 0.7) \quad (A13)$

$PLMXP_a$ , potential maximum photosynthetic rate ( $\text{mg CO}_2 \text{ m}^{-2} \text{ s}^{-1}$ );  $F_{CO_2}$ , enhancement of photosynthetic rate due to  $\text{CO}_2$  (-);  $[CO_2]_A$ , atmospheric  $\text{CO}_2$  concentration (ppm);  $N_L$ , leaf N concentration ( $\text{g N m}^{-2}$ );  $DS$ , development stage (-);  $DRV$ , development rate during the vegetative stage ( $\text{day}^{-1}$ );  $DRR$ , development rate during the reproductive stage ( $\text{day}^{-1}$ );  $DRCV$ , development rate constant during the vegetative stage ( $\text{day}^{-1}$ );  $DRCR$ , development rate constant during the reproductive stage ( $\text{day}^{-1}$ );  $T_A$ , daily average air temperature ( $^{\circ}\text{C}$ );  $CASST$ , fraction of available C allocated to aboveground biomass (-);  $CALVT$ , fraction of available C allocated to leaves (-);  $CASTT$ , fraction of available C allocated to stems (-);  $EXD$ , exudation rate ( $\text{mg C m}^{-2} \text{ day}^{-1}$ );  $DW_{\text{root}}$ , root dry weight ( $\text{g m}^{-2}$ );  $RTL$ , root litter rate ( $\text{g C m}^{-2} \text{ day}^{-1}$ );  $BM_{\text{root}}$ , root biomass ( $\text{g C m}^{-2}$ );  $N_{\text{tiller}}$ , rice tiller density ( $\text{m}^{-2}$ );  $N_{\text{tiller}}^0$ , initial tiller density ( $\text{m}^{-2}$ );  $HUT$ , heat units ( $^{\circ}\text{C day}$ ); and  $T_W$ , daily mean temperature of the flood water ( $^{\circ}\text{C}$ ).

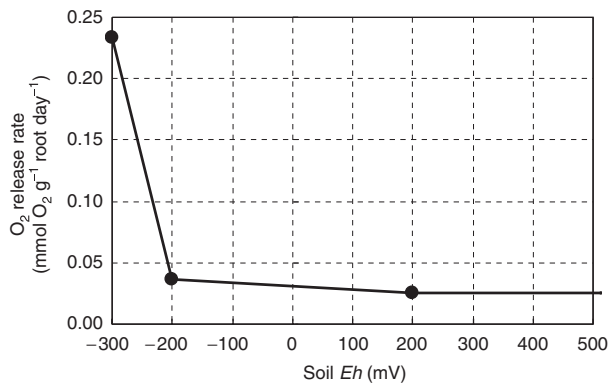


**Fig. A1** The function used in the revised DNDC model to calculate the oxygen release rate from rice roots as a function of soil redox potential (*Eh*).

ments (Wang & Adachi, 2000). Root respiration releases CO<sub>2</sub> into the soil. Oxygen release from rice roots is simulated using a function that relates the O<sub>2</sub> release rate to soil *Eh* (Fig. A1) that was derived from experimental data (Kludze *et al.*, 1993).

### Soil biogeochemistry submodel

The major functions of the soil biogeochemistry submodel are summarized in Table A2. Most parameters in the functions were adopted from published research, but several were assumed, calibrated, or determined in the present study, as identified in the table.

At the beginning of each day in the simulation sequence, this submodel calculates decomposition of

**Table A2** Major functions used in the soil biogeochemistry submodel of the revised DNDC model

Function	Equation
Decomposition of C pools	$\frac{d}{dt}[C] = -SDR[C]f_T f_M f_N f_{O_2} f_{clay} f_{tillage} DRF \quad (A14)$
	$f_T^*, f_M^*, f_N^* : \text{see Fig. A2}$
	$f_{O_2} = 0.2 + 0.8[O_2]/[O_2]_{sat}^* \quad (A15)$
	$f_{clay} = \max(0, 1 - 1.2 \text{ clay})^* \quad (A16)$
	$f_{tillage} = \max(1, 1.75 - 0.01 \text{ DATL})^* \quad (A17)$
	$DRF = 0.6^\dagger \quad (A18)$
Reduction of oxides Fe <sup>3+</sup> and Mn <sup>4+</sup> reduction SO <sub>4</sub> <sup>2-</sup> reduction	$RED = V_{max} \frac{[A]}{K_A + [A]} \cdot \frac{[D]}{K_D + [D]} Q_{10}^{\frac{T-30}{10}} \quad (A19)$
	$V_{max} = 4.5 \text{ (mmol kg}^{-1} \text{ h}^{-1}) \quad (A20)$
	$K_A = 0.15 \text{ (mol kg}^{-1}) \quad (A21)$
	$K_D = 0.46 \text{ (mol m}^{-3}) \text{ for DOC, } 0.22 \text{ (mmol m}^{-3}) \text{ for H}_2 \quad (A22)$
	$Q_{10} = 2.4(-) \quad (A23)$
	$V_{max} = 2.88 \times 10^{-2} \text{ (mol m}^{-3} \text{ h}^{-1}) \quad (A24)$
	$K_A = 0.23 \text{ (mol m}^{-3}) \quad (A25)$

*Continued*

Table A2. (Contd.)

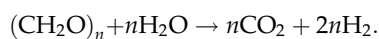
Function	Equation
	$K_D = 1.6 \text{ (mol m}^{-3}\text{) for DOC, } 2.87 \text{ (mmol m}^{-3}\text{) for H}_2$ (A26)
	$Q_{10} = 1.6 \text{ (-)}$ (A27)
Oxidation of $\text{Mn}^{2+}$ , $\text{Fe}^{2+}$ , and $\text{H}_2\text{S}$	$OXD = 0.004[R] \text{ ([O}_2\text{]} > 0)$ (A28)
Soil $Eh$ (see Fig. A3)	$Eh = \begin{cases} -189.1 - 310.8 \log([\text{Fe}^{2+}]/[\text{Fe}_{\text{red}}]) & (-180 < Eh \leq 300) \\ -220.5 - 131.8 \log([\text{H}_2\text{S}]/[\text{S}_{\text{red}}]) & (Eh \leq -180) \end{cases}$ (A29)
$\text{CH}_4$ production	$PRD_{\text{CH}_4} = 0.18 \frac{[D]}{K_D + [D]} (4.6)^{\frac{T-30}{10}}$ (A30)
	$K_D = 1.6 \text{ (mol m}^{-3}\text{) for DOC, } 2.87 \text{ (mmol m}^{-3}\text{) for H}_2$ (A31)
$\text{CH}_4$ oxidation	$OXD_{\text{CH}_4} = 0.13 \frac{[\text{CH}_4]}{0.045 + [\text{CH}_4]} \cdot \frac{[\text{O}_2]}{0.033 + [\text{O}_2]} (2.0)^{\frac{T-25}{10}}$ (A32)
$\text{CH}_4$ emission	$EMS_{\text{CH}_4} = D_{\text{tiller}} N_{\text{tiller}} [\text{CH}_4]$ (A33) $D_{\text{tiller}}$ : see Fig. A4.

\*Assumed in this study.

†Calibrated using field observations in this study.

[C], organic C pool of residues, microbial biomass, or humads ( $\text{kg C ha}^{-1}$ );  $SDR$ , specific decomposition rate ( $\text{day}^{-1}$ );  $f_T$ ,  $f_M$ ,  $f_N$ ,  $f_{O_2}$ ,  $f_{\text{clay}}$ , and  $f_{\text{tillage}}$  effects of soil temperature, moisture, N deficiency,  $\text{O}_2$  concentration, clay content, and tillage (-);  $[\text{O}_2]$ ,  $\text{O}_2$  concentration in soil water ( $\text{mol m}^{-3}$ );  $[\text{O}_2]_{\text{sat}}$ , saturated  $\text{O}_2$  concentration in soil water ( $\text{mol m}^{-3}$ );  $\text{clay}$ , clay content ( $\text{g g}^{-1}$ );  $DATL$ , days after tillage (day);  $DRE$ , field decomposition reduction factor (-);  $RED$ , reduction rate ( $\text{mol kg}^{-1} \text{h}^{-1}$  or  $\text{mol m}^{-3} \text{h}^{-1}$ );  $V_{\text{max}}$ , maximum reaction rate at a reference temperature;  $K_A$ , half saturation constant for electron acceptors;  $K_D$ , half saturation constant for electron donors;  $[D]$ , concentration of electron donors;  $[A]$ , concentration of electron acceptors;  $T$ , soil temperature ( $^{\circ}\text{C}$ );  $OXD$ , oxidation rate ( $\text{mol kg}^{-1} \text{h}^{-1}$ );  $[R]$ , concentration of the reduced species ( $\text{mol kg}^{-1}$ );  $Eh$ , redox potential of the soil (mV);  $[\text{Fe}_{\text{red}}]$ , concentration of reducible Fe ( $\text{mol kg}^{-1}$ );  $[\text{S}_{\text{red}}]$ , concentration of reducible S ( $\text{mol kg}^{-1}$ );  $PRD_{\text{CH}_4}$ , rate of  $\text{CH}_4$  production ( $\text{mmol kg}^{-1} \text{h}^{-1}$ );  $OXD_{\text{CH}_4}$ , rate of  $\text{CH}_4$  oxidation ( $\text{mol m}^{-3} \text{h}^{-1}$ );  $[\text{CH}_4]$ ,  $\text{CH}_4$  concentration in soil water ( $\text{mol m}^{-3}$ );  $EMS_{\text{CH}_4}$ , rate of  $\text{CH}_4$  emission through rice tillers ( $\text{mol m}^{-2} \text{h}^{-1}$ );  $D_{\text{tiller}}$ , conductance of rice tillers for  $\text{CH}_4$  diffusion ( $\text{m}^3 \text{h}^{-1} \text{tiller}^{-1}$ ); and  $N_{\text{tiller}}$ , tiller density ( $\text{m}^{-2}$ ).

organic C pools (plant residues, microbial biomass, and humads). The decomposition rate is calculated using first-order reaction kinetics based on the effects of soil moisture, temperature, clay content,  $\text{O}_2$  concentration, N deficiency, and tillage practice. In this model, N deficiency is defined as the ratio of N demand to N supply. When organic C is decomposed under anaerobic conditions, it is assumed that  $\text{H}_2$  is produced according to the following reaction:



Among the kinetic parameters used to calculate decomposition, the  $SDR$  and the N deficiency factor were

derived from values in the literature (Molina *et al.*, 1983; Gilmour *et al.*, 1985), whereas the others were calibrated or assumed in this study.

Reduction of  $\text{Fe}^{3+}$ ,  $\text{Mn}^{4+}$ , and  $\text{SO}_4^{2-}$  in anaerobic soil is calculated using dual-substrate Michaelis–Menten kinetics based on the concentrations of electron donors and acceptors and on soil temperature. When  $\text{O}_2$  is available in the soil, oxidation of  $\text{Fe}^{2+}$ ,  $\text{Mn}^{2+}$ , and  $\text{H}_2\text{S}$  is calculated using first-order kinetics. The redox potential ( $Eh$ ) of anaerobic soil is estimated using empirical functions that relate soil  $Eh$  to  $\text{Fe}^{3+}$  and  $\text{SO}_4^{2-}$  reduction, derived from soil incubation data (Takai *et al.*, 1957; Takai, 1961a–c). Methane production is calculated using Michaelis–Menten kinetics based on electron donor

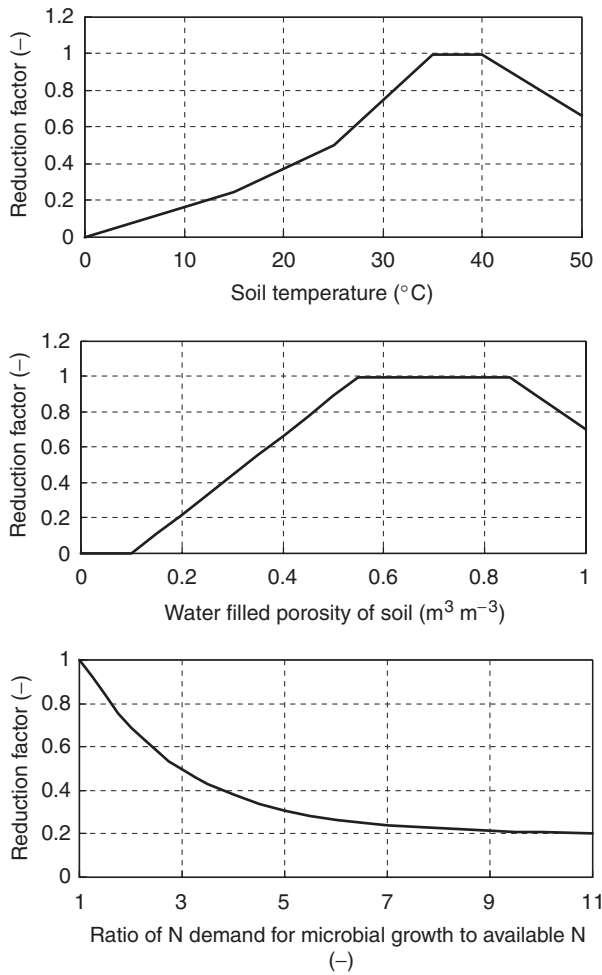


**Fig. A2** Reduction factors for decomposition rate as a function of soil temperature (upper graph), soil moisture (middle graph), and N deficiency (lower graph) in the revised DNDC.

concentrations and soil temperature. When O<sub>2</sub> is available, CH<sub>4</sub> oxidation is calculated using dual-substrate Michaelis–Menten kinetics based on CH<sub>4</sub> and O<sub>2</sub> concentrations and on soil temperature. We adopted values of parameters for soil reduction and CH<sub>4</sub> production and oxidation from the research literature (Watson *et al.*, 1997; Van Bodegom & Stams, 1999; Van Bodegom & Scholten, 2001). Parameters for the oxidation of Fe<sup>2+</sup>, Mn<sup>2+</sup>, and H<sub>2</sub>S were estimated based on field observation data from Gotoh & Yamashita (1966). After fertilization, we assumed a first-order dissolution rate constant of 0.5 day<sup>-1</sup> for both urea and (NH<sub>4</sub>)<sub>2</sub>SO<sub>4</sub>, and assumed that dissolved SO<sub>4</sub><sup>2-</sup> is added to the soil SO<sub>4</sub><sup>2-</sup> pool.

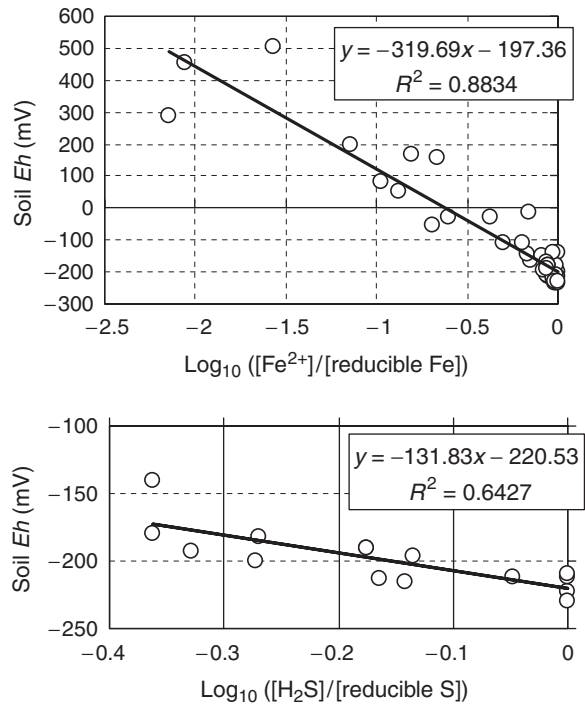


**Fig. A3** Empirical equations relating soil Eh to Fe and S reduction in anaerobic soils, derived from published data from soil incubation experiments.

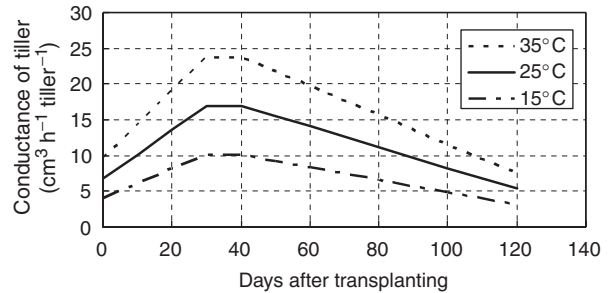


**Fig. A4** The function used in the revised DNDC model to estimate the conductance of rice tillers for CH<sub>4</sub> as a function of plant age and soil temperature.

Methane emission through rice plants to the atmosphere is simulated using a diffusion model that assumes CH<sub>4</sub> emission is driven by the CH<sub>4</sub> concentration gradient between the soil solution and the atmosphere. The conductance of a single rice tiller for CH<sub>4</sub> diffusion is estimated using a function that relates the conductance to rice age and soil temperature (Fig. A4), which was derived from laboratory measurements (Hosono & Nouchi, 1997).